Nuclear Partition Functions at Temperatures Exceeding 10^{10} K

T. Rauscher

Departement für Physik und Astronomie, Universität Basel, 4056 Basel, Switzerland

Thomas.Rauscher@unibas.ch

ABSTRACT

Nuclear partition functions were calculated for a grid of temperatures from 1.2×10^{10} K to 2.75×10^{11} K ($1 \leq kT \leq 24$ MeV) within a Fermi-gas approach, including all nuclides from the proton-dripline to the neutron-dripline with proton number $9 \leq Z \leq 85$. The calculation is based on a nuclear level density description published elsewhere, thus extending the previous tables of partition functions beyond 10^{10} K. Additional high temperature corrections had to be applied.

Subject headings: nuclear reactions, nucleosynthesis, abundances

1. Introduction

The knowledge of the nuclear partition function at high temperatures is essential in understanding the nuclear equation of state used in the core collapse phase of massive stars. In self-consistent simulations, the contraction of the core is explicitly followed up to nuclear densities, giving rise to extreme temperatures and high mean excitation energies of the nuclei. Ratios of high temperature partition functions are also ingredients in nucleosynthesis networks in explosive scenarios, such as the r- and rp-processes. When employed in nuclear statistical equilibria (NSE), they often have to be known at temperatures beyond 10^{10} K.

Recently, new sets of partition functions have been published along with astrophysical reaction rates for nuclides from proton dripline to neutron dripline and charge number $10 \leq Z \leq 85$ (Rauscher & Thielemann 2000). The sets include partition functions up to $T_9 = 10$ (10^{10} K) based on two different level densities calculated within a shifted Fermi-gas approach (Rauscher et al. 1997) utilizing two mass formulas. Here, the extension of these partition functions to temperatures of $T_9 = 275$ is presented. A straightforward extrapolation is not valid because of additional effects acting at high temperatures.

These effects have been a matter of discussion already about 20 years ago (Fowler, Engelbrecht, & Woosley 1978; Mazurek, Lattimer, & Brown 1979). The recently improved descriptions of nuclear level density and nuclear reaction rate predictions make it worthwhile to reconsider these arguments and to publish a complete table of partition functions. In this work, in addition to using the more recent level densities of Rauscher et al. (1997), the corrections are treated by closely following Tubbs & Koonin (1979).

2. Procedure

The temperature-dependent partition function $G(T)$ normalized to the ground state spin of the nucleus J^0 is usually defined as (Fowler et al. 1967)

$$(2J^0 + 1)G(T) = \sum_{\mu=0}^{\mu_m}(2J^\mu + 1)e^{-E^\mu/kT} \tag{1}$$
$$+ \int_{E^{\mu_m}}^{E^{\max}} \sum_{J^\mu,\pi^\mu}(2J^\mu + 1)e^{-\epsilon/kT}\rho(\epsilon, J^\mu, \pi^\mu)d\epsilon \quad ,$$

with ρ being the level density and μ_m the label of the last included experimentally known state. The sum over Boltzmann-weighted discrete states from the ground state to state μ_m is performed using experimental levels as listed in Rauscher & Thielemann (2001). Above the last known state an integration over the nuclear level density is used instead of a summation, as also outlined in Rauscher & Thielemann (2000), employing the level density description of Rauscher et al. (1997).

The upper limit $E^{\max}$ of the integration requires special consideration. Formally, the integration procedure should encompass energies up to infinity. However, for all practical purposes an energy cut-off can be introduced because the Boltzmann-factor $e^{-\epsilon/kT}$ dominates at high energies and suppresses any further contributions to the integral value. It is well known that, for instance, the maximum excitation energy above which there are no more significant contributions to the partition function is of the order of $20-25$ MeV up to $T_9 = 10$ (Rauscher & Thielemann 2000).

Due to the temperature dependence of the integrand in Eq. 1 its peak contribution is shifted to higher energies for higher temperatures T, thus also requiring a larger cut-off $E^{\max}$. Up to now, there has been no systematic scrutiny of the behavior of the integrand, which also weakly depends on the used level density. In Fig. 1, the integrands are plotted, also showing the peak energies and the widths of the peaks for different energies. The shown energies are in agreement with the mean excitation energies derived by Tubbs & Koonin (1979). In the

same manner, the cut-off energy of 25 MeV, often used for calculating partition functions up to $T_9 = 10$, can be justified.

For $T_9 > 12$, we extract a (nearly) quadratic dependence on temperature of the peak energy E_{peak} and a linear dependence of the width Γ_{FWHM} of the integrand:

$$
\begin{aligned}
E_{\text{peak}} &= 0.0725 T_9^{2.055} \quad \text{MeV}, \\
\Gamma_{\text{FWHM}} &= 3T_9 - 37.0 \quad \text{MeV}.
\end{aligned}
\tag{2}
$$

The integration cut-off was then set to $E^{\text{max}} = \max\left(35, E_{\text{peak}} + \Gamma_{\text{FWHM}}\right)$ MeV.

3. High temperature corrections

Due to the exponential increase of the nuclear level density with excitation energy, extremely large partition functions already result at temperatures of a few MeV (temperatures given as energies and in T_9 are related by $E = T_9/11.6045$ MeV). However, it has been realized that a straightforward integration over the level density might overestimate the partition functions. High excitation energies of the nucleus permit the emission of nucleons and therefore an appropriate fraction of the level density associated with such continuum states should be neglected in the computation of the partition function.

Fowler, Engelbrecht, & Woosley (1978) introduced such high temperature corrections by truncating the integration near the nucleon separation energy and by subtracting continuum scattering states (which, however, do not act below $T_9 = 100$). Mazurek, Lattimer, & Brown (1979) accounted for the suppression of the partition functions by arbitrarily setting the integral cut-off to 25 MeV. In a semi-classical calculation, Tubbs & Koonin (1979) showed that Fowler, Engelbrecht, & Woosley (1978) and Mazurek, Lattimer, & Brown (1979) largely overestimated the suppression, that a simple truncation of the integral is incorrect, and that partition functions remain large for temperatures as high as $T_9 = 100$. They find that the corrections are much smaller than given by truncated level density integrals and that the conventional partition functions (with full integration) are much closer to their values than values obtained with any of the truncation methods.

The advantage of the description by Tubbs & Koonin (1979), which is based on the independent particle model, is the natural inclusion of both bound and continuum nuclear states. Here, we use a hybrid model by using the level density and partition function descriptions as outlined in Sec. 2 and applying correction factors derived from the spherical square well approximation of Tubbs & Koonin (1979) (Eqs. 7 and 9 in that reference) but using the same nuclear properties (nucleon separation energies, nuclear radius) as in Rauscher &

Thielemann (2000). This way, a continuous extension of the partition functions of Rauscher & Thielemann (2000) is possible. While the simplicity of the equations is kept, the limitations of the spherical square well approach are partially lifted because, e.g., the separation energies are taken from experiment or from mass formulas employing more realistic nuclear potentials and accounting for shell and deformation effects. Furthermore, this approach is only used to obtain the relative corrections.

The correction factor C is extracted by comparing the uncorrected and the corrected total nuclear partition function of Tubbs & Koonin (1979) computed in their spherical square well formalism. While referring the reader to the paper of Tubbs & Koonin (1979) for a more complete description of their approach, only the relevant equations are summarized here. The total nuclear partition function $Z = Z_{\mathrm{esw}} = (2J_i^0 + 1)G_{\mathrm{esw}}(T)$ is constructed as the sum of two terms for protons and neutrons, respectively:

$$\ln Z = \ln Z_p + \ln Z_n \quad , \tag{3}$$

with

$$\ln Z_x = \ln q_x - \alpha X + \beta E_{0x} - \frac{1}{2}\ln(2\pi\mathfrak{N}) \quad . \tag{4}$$

The letter x stands for neutron (n) and proton (p), respectively, and X is the neutron number N and the proton number Z, respectively. The ground state energy is denoted by E_{0x} and the inverse nuclear temperature by $\beta = 1/kT$ with $\beta = 11.6045/T_9$ MeV. The mean-square number fluctuation $\mathfrak{N}$, the nuclear contribution q_x (as opposed to the contribution of the exterior nucleon gas) of the grand partition function, and the Lagrange multiplier α can be found with and without continuum contributions, leading to nucleon partition functions Z_x, Z_x' and total partition functions Z, Z' with and without corrections. In the following, primed quantities are without corrections. Thus, we obtain

$$q_x' = D(T)\left[F_{3/2}\left(\alpha' + \beta S_x + 3\beta X/2\rho_F\right)\right] \quad ,$$
$$q_x = D(T)\left[F_{3/2}\left(\alpha + \beta S_x + 3\beta X/2\rho_F\right) - F_{3/2}\left(\alpha\right)\right] \quad , \tag{5}$$

and

$$\mathfrak{N}' = \frac{3}{4}D(T)\left[F_{-1/2}\left(\alpha' + \beta S_x + 3\beta X/2\rho_F\right)\right] \quad ,$$
$$\mathfrak{N} = \frac{3}{4}D(T)\left[F_{-1/2}\left(\alpha + \beta S_x + 3\beta X/2\rho_F\right) - F_{-1/2}\left(\alpha\right)\right] \quad . \tag{6}$$

Fermi integrals of the order η with argument θ are denoted by $F_\eta(\theta)$. The factor $D(T)$ is

$$D(T) = \frac{1}{\sqrt{X}}\left(\frac{2\rho_F kT}{3}\right)^{\frac{3}{2}} \quad . \tag{7}$$

For consistency, the same particle separation energy S_x is used as for the reaction rate calculations of Rauscher & Thielemann (2000). It is taken either from experiment or from a mass formula where no experimental information is available. The level density at the zero-temperature Fermi surface is given as

$$\rho_F = \left(\frac{4}{\sqrt{3\pi}}\right)^{\frac{2}{3}} X^{\frac{1}{3}} \frac{m_x R^2}{\hbar^2} \quad , \tag{8}$$

using the nuclear radius R and the nucleon mass m_x. With that definition the ground state energy becomes

$$E_{0x} = -\frac{3}{5}\frac{X^2}{\rho_F} - X S_x \quad . \tag{9}$$

Before evaluating the above equations, the appropriate (temperature dependent) Lagrange multiplicators with and without corrections have to be determined. This is done by requiring states in the grand canonical ensemble to have, on the average, the correct number of nucleons, X, and therefore by finding the root of the following equations with respect to α and α':

$$\begin{aligned}
\tfrac{3}{2}D(T)\left[F_{1/2}\left(\alpha' + \beta S_x + 3\beta X/2\rho_F\right)\right] - X &= 0 \quad , \\
\tfrac{3}{2}D(T)\left[F_{1/2}\left(\alpha + \beta S_x + 3\beta X/2\rho_F\right) - F_{1/2}\left(\alpha\right)\right] - X &= 0 \quad .
\end{aligned} \tag{10}$$

The proper α or α' found above has to be inserted also in Eq. 4, of course.

Finally, the relevant partition function $\overline{G}(T)$ is then obtained by multiplying the previous function (from Sec. 2) with the correction C:

$$\overline{G}(T) = C(T)G(T) = \exp\left(\ln Z(T) - \ln Z'(T)\right) G(T) \quad . \tag{11}$$

Thus, the correction factor C found with the approach above is applied to the partition function derived in the full computation described in Sec. 2. The corrections start to act at temperatures $T_9 \simeq 50 - 60$ for light and intermediate nuclei and as low as $T_9 \simeq 14$ for heavy nuclei. Corrections are negligible for $T_9 \leq 10$, implying that the partition functions from Rauscher & Thielemann (2000) can be used without further modifications. The magnitude of the corrections ranges from a few percent at the lower end of the temperature range to a suppression factor of 10^{-5} for the heaviest nuclides at $T_9 = 100$ and 10^{-40} at $T_9 = 275$, respectively. The correction factors for a few selected cases are shown in Table 1.

4. Discussion and Conclusion

The corrected renormalized partition functions $\overline{G}$ calculated with level densities utilizing input from the Finite Range Droplet Model (FRDM) (Möller et al. 1995) (see also Rauscher

& Thielemann 2000) are given in Table 2. Results making use of the Extended Thomas-Fermi mass formula with shell quenching effects (ETFSI-Q) (Pearson et al. 1996) (see also Rauscher & Thielemann 2000) far from stability are given in Table 3. The properties of the mass formulas can enter via the particle separation energies which are calculated from predicted mass differences in case no experimental masses are known. Furthermore, they always enter in the microscopic correction term used in the level density treatment of Rauscher et al. (1997). The method to calculate the high temperature corrections is only applicable for bound nucleons, therefore only those nuclides are given for which both the neutron and proton separation energies are positive. The printed version of this paper contains only example tables, showing which kind of information is available. Partition functions for the full range of nuclides from proton dripline to neutron dripline for $10 \leq Z \leq 83$ (FRDM) and $26 \leq Z \leq 85$ (ETFSI-Q) are available as machine readable tables in electronic form. The formatting is the same as used in Rauscher & Thielemann (2000), except for the different temperature range. Thus, the partition functions presented here provide a smooth and analytical extension of the previous tabulation, extending the range of temperatures to $0.1 \leq T_9 \leq 275$.

The new values for ^{56}Ni can directly be compared to the ones from Tubbs & Koonin (1979). Fig. 2 shows the partition function of this nucleus. By comparing to Fig. 1 in Tubbs & Koonin (1979) it can be seen that the new value is higher by 45–50% around $kT = 10$ MeV than their corrected value B. This is mainly due to the different level density description (different effective level density parameter a) used since a similar treatment of the high-temperature corrections is implemented in both calculations.

It has to be noted that the partition functions presented here are valid for low-density conditions. In high-density regimes, modifications of nuclear properties (e.g., separation energies) might have to be additionally applied. This is beyond the scope of the current investigation.

The nuclear model for the corrections (and the one for the level density) assumes a Fermi-gas of independent nucleons interacting only through a common, spin-independent mean field. At nuclear temperatures beyond about 30 MeV (i.e. $T_9 \geq 350$), the momentum dependence of the mean field, the excitation of mesonic degrees of freedom, and the breakdown of the independent particle approximation become important. This is not relevant for the temperature range explored here but will necessitate an altogether different approach when expanding the temperature range beyond about 25–30 MeV. It is expected that the exponential rise of the partition functions with temperature will finally be effectively suppressed beyond those energies.

REFERENCES

Fowler, W.A., Caughlan, G.R., and Zimmermann, B.A. 1967, ARA&A, 5, 525

Fowler, W. A., Engelbrecht, C. A., & Woosley, S. E. 1978, ApJ, 226, 984

Mazurek, T. J., Lattimer, J. M., & Brown, G. E. 1979, ApJ, 223, 314

Möller, P., Nix, J. R., Myers, W. D., & Swiatecki, W. J. 1995, At. Data Nucl. Data Tables, 59, 185

Pearson, J. M., Nayak, R. C., & Goriely, S. 1996, Phys. Lett. B, 387, 455

Rauscher, T., & Thielemann, F.-K. 2000, At. Data Nucl. Data Tables, 75, 1; also available at http://nucastro.org/reaclib.html

Rauscher, T., & Thielemann, F.-K. 2001, At. Data Nucl. Data Tables, 79, 47; also available at http://nucastro.org/reaclib.html

Rauscher, T., Thielemann, F.-K., & Kratz, K.-L. 1997, Phys. Rev. C, 56, 1613

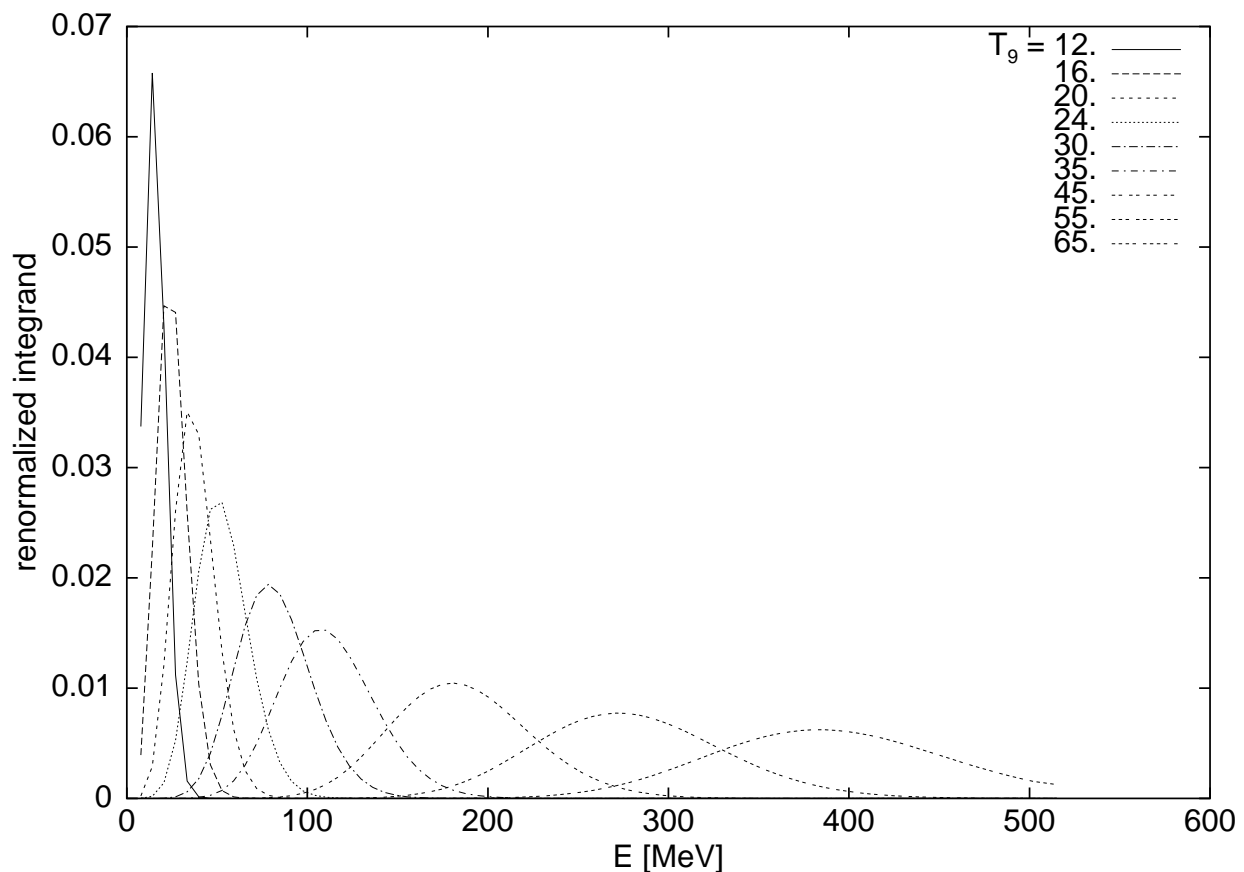Tubbs, D. L., & Koonin, S. E. 1979, ApJ, 232, L59

Fig. 1.— Integrands from Eq. 1 for different temperatures T_9 of ^{109}Cd. The absolute values are renormalized so that the area under the curves is the same. It can be seen that for increasing temperature the location of the peak, arising from folding the Boltzmann factor $e^{-E/kT}$ with the level density $\rho(E)$, is shifted to increasingly higher excitation energies E. At the same time, the width of the peak is increased, thus allowing significant contributions to the integral at even higher energies.
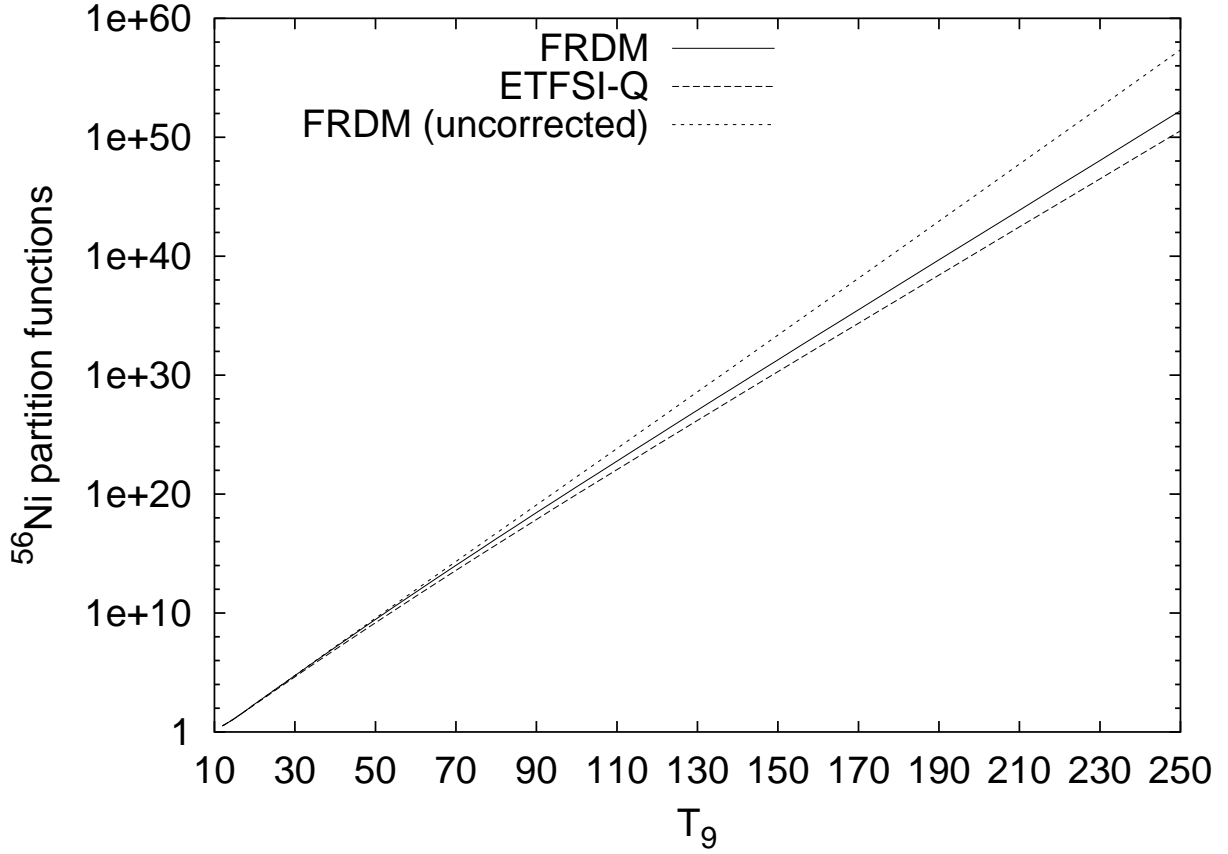
Fig. 2.— Partition function of ^{56}Ni calculated with level densities including inputs from FRDM (full line) and ETFSI-Q (dashed line). Both calculations include high-temperature corrections which, however, become significant only at $kT > 5$ MeV for this nucleus. Differences between FRDM and ETFSI-Q partition functions are more pronounced for neutron-rich nuclides. Also shown is a partition function without the continuum corrections (dotted line).

Table 1.   Correction factors $C(T_9)$ for selected cases. Numbers in square brackets denote powers of ten.

Nuclide							
$C(12)$	$C(14)$	$C(16)$	$C(18)$	$C(20)$	$C(22)$	$C(24)$	$C(26)$
$C(28)$	$C(30)$	$C(35)$	$C(40)$	$C(45)$	$C(50)$	$C(55)$	$C(60)$
$C(65)$	$C(70)$	$C(75)$	$C(80)$	$C(85)$	$C(90)$	$C(95)$	$C(100)$
$C(110)$	$C(130)$	$C(150)$	$C(170)$	$C(190)$	$C(210)$	$C(230)$	$C(250)$
^{16}O							
1.00[+00]	1.00[+00]	1.00[+00]	1.00[+00]	1.00[+00]	1.00[+00]	1.00[+00]	1.00[+00]
9.99[−01]	9.99[−01]	9.97[−01]	9.93[−01]	9.87[−01]	9.78[−01]	9.65[−01]	9.49[−01]
9.29[−01]	9.05[−01]	8.79[−01]	8.49[−01]	8.17[−01]	7.83[−01]	7.48[−01]	7.11[−01]
6.36[−01]	4.90[−01]	3.63[−01]	2.61[−01]	1.83[−01]	1.27[−01]	8.66[−02]	5.89[−02]
^{56}Fe							
1.00[+00]	1.00[+00]	1.00[+00]	1.00[+00]	9.99[−01]	9.98[−01]	9.96[−01]	9.93[−01]
9.88[−01]	9.82[−01]	9.60[−01]	9.24[−01]	8.75[−01]	8.14[−01]	7.42[−01]	6.64[−01]
5.83[−01]	5.03[−01]	4.26[−01]	3.55[−01]	2.90[−01]	2.34[−01]	1.86[−01]	1.46[−01]
8.69[−02]	2.71[−02]	7.50[−03]	1.90[−03]	4.56[−04]	1.06[−04]	2.40[−05]	5.43[−05]
^{56}Ni							
1.00[+00]	1.00[+00]	9.99[−01]	9.98[−01]	9.96[−01]	9.92[−01]	9.88[−01]	9.82[−01]
9.74[−01]	9.65[−01]	9.33[−01]	8.90[−01]	8.35[−01]	7.71[−01]	7.00[−01]	6.24[−01]
5.48[−01]	4.73[−01]	4.02[−01]	3.36[−01]	2.78[−01]	2.26[−01]	1.81[−01]	1.44[−01]
8.72[−02]	2.86[−02]	8.33[−03]	2.23[−03]	5.61[−04]	1.36[−04]	3.24[−05]	7.63[−06]
^{176}Hf							
9.99[−01]	9.97[−01]	9.93[−01]	9.85[−01]	9.72[−01]	9.52[−01]	9.26[−01]	8.92[−01]
8.51[−01]	8.04[−01]	6.61[−01]	5.05[−01]	3.57[−01]	2.33[−01]	1.42[−01]	8.07[−02]
4.29[−02]	2.15[−02]	1.01[−02]	4.54[−03]	1.93[−03]	7.88[−04]	3.08[−04]	1.16[−04]
1.49[−05]	1.77[−07]	1.55[−09]	1.12[−11]	7.28[−14]	4.51[−16]	2.79[−18]	1.77[−20]
^{208}Pb							
9.99[−01]	9.97[−01]	9.93[−01]	9.84[−01]	9.69[−01]	9.48[−01]	9.18[−01]	8.80[−01]
8.34[−01]	7.80[−01]	6.23[−01]	4.55[−01]	3.03[−01]	1.85[−01]	1.03[−01]	5.32[−02]
2.53[−02]	1.12[−02]	4.64[−03]	1.80[−03]	6.62[−04]	2.30[−04]	7.61[−05]	2.41[−05]
2.14[−06]	1.15[−08]	4.30[−11]	1.28[−13]	3.36[−16]	8.33[−19]	2.06[−21]	5.24[−24]

Note. — The values given here were calculated with separation energies based on experiment or FRDM input (see text).

Table 2. Renormalized partition functions $\overline{G}(T_9)$ including high temperature corrections. The values given here were calculated with level densities based on FRDM input (see text). Each nuclide is characterized by its charge and mass numbers Z, A, and its ground-state spin J^0. Numbers in square brackets denote powers of ten.

Nuclide							
Z	A	J^0					
$\overline{G}(12)$	$\overline{G}(14)$	$\overline{G}(16)$	$\overline{G}(18)$	$\overline{G}(20)$	$\overline{G}(22)$	$\overline{G}(24)$	$\overline{G}(26)$
$\overline{G}(28)$	$\overline{G}(30)$	$\overline{G}(35)$	$\overline{G}(40)$	$\overline{G}(45)$	$\overline{G}(50)$	$\overline{G}(55)$	$\overline{G}(60)$
$\overline{G}(65)$	$\overline{G}(70)$	$\overline{G}(75)$	$\overline{G}(80)$	$\overline{G}(85)$	$\overline{G}(90)$	$\overline{G}(95)$	$\overline{G}(100)$
$\overline{G}(105)$	$\overline{G}(110)$	$\overline{G}(115)$	$\overline{G}(120)$	$\overline{G}(125)$	$\overline{G}(130)$	$\overline{G}(135)$	$\overline{G}(140)$
$\overline{G}(145)$	$\overline{G}(150)$	$\overline{G}(155)$	$\overline{G}(160)$	$\overline{G}(165)$	$\overline{G}(170)$	$\overline{G}(175)$	$\overline{G}(180)$
$\overline{G}(190)$	$\overline{G}(200)$	$\overline{G}(210)$	$\overline{G}(220)$	$\overline{G}(230)$	$\overline{G}(240)$	$\overline{G}(250)$	$\overline{G}(275)$
^{56}Ni							
28	56	0.0					
3.23[+00]	8.19[+00]	2.37[+01]	7.17[+01]	2.19[+02]	6.64[+02]	2.01[+03]	6.08[+03]
1.83[+04]	5.52[+04]	8.60[+05]	1.31[+07]	1.96[+08]	2.86[+09]	4.06[+10]	5.63[+11]
7.64[+12]	1.02[+14]	1.33[+15]	1.71[+16]	2.17[+17]	2.71[+18]	3.35[+19]	4.10[+20]
4.96[+21]	5.94[+22]	7.05[+23]	8.30[+24]	9.71[+25]	1.13[+27]	1.30[+28]	1.50[+29]
1.71[+30]	1.94[+31]	2.20[+32]	2.49[+33]	2.80[+34]	3.14[+35]	3.51[+36]	3.93[+37]
4.87[+39]	6.02[+41]	7.41[+43]	9.11[+45]	1.12[+48]	1.38[+50]	1.70[+52]	2.90[+57]

Note. — The complete version of this table can be found in the electronic edition of Astrophysical Journal Supplement. The printed edition contains only a sample of what kind of information is given. The full tables can also be downloaded from http://ftp.nucastro.org/astro/fits/partfuncs/.

Table 3. Renormalized partition functions $\overline{G}(T_9)$ including high temperature corrections. The values given here were calculated with level densities based on ETFSI-Q input (see text). Each nuclide is characterized by its charge and mass numbers Z, A, and its ground-state spin J^0. Numbers in square brackets denote powers of ten.

Nuclide							
Z	A	J^0					
$\overline{G}(12)$	$\overline{G}(14)$	$\overline{G}(16)$	$\overline{G}(18)$	$\overline{G}(20)$	$\overline{G}(22)$	$\overline{G}(24)$	$\overline{G}(26)$
$\overline{G}(28)$	$\overline{G}(30)$	$\overline{G}(35)$	$\overline{G}(40)$	$\overline{G}(45)$	$\overline{G}(50)$	$\overline{G}(55)$	$\overline{G}(60)$
$\overline{G}(65)$	$\overline{G}(70)$	$\overline{G}(75)$	$\overline{G}(80)$	$\overline{G}(85)$	$\overline{G}(90)$	$\overline{G}(95)$	$\overline{G}(100)$
$\overline{G}(105)$	$\overline{G}(110)$	$\overline{G}(115)$	$\overline{G}(120)$	$\overline{G}(125)$	$\overline{G}(130)$	$\overline{G}(135)$	$\overline{G}(140)$
$\overline{G}(145)$	$\overline{G}(150)$	$\overline{G}(155)$	$\overline{G}(160)$	$\overline{G}(165)$	$\overline{G}(170)$	$\overline{G}(175)$	$\overline{G}(180)$
$\overline{G}(190)$	$\overline{G}(200)$	$\overline{G}(210)$	$\overline{G}(220)$	$\overline{G}(230)$	$\overline{G}(240)$	$\overline{G}(250)$	$\overline{G}(275)$
^{56}Ni							
28	56	0.0					
3.20[+00]	8.03[+00]	2.28[+01]	6.76[+01]	2.01[+02]	5.94[+02]	1.74[+03]	5.10[+03]
1.48[+04]	4.30[+04]	6.08[+05]	8.43[+06]	1.14[+08]	1.52[+09]	1.97[+10]	2.50[+11]
3.11[+12]	3.80[+13]	4.56[+14]	5.40[+15]	6.30[+16]	7.25[+17]	8.25[+18]	9.29[+19]
1.04[+21]	1.14[+22]	1.25[+23]	1.36[+24]	1.47[+25]	1.57[+26]	1.67[+27]	1.77[+28]
1.87[+29]	1.96[+30]	2.06[+31]	2.14[+32]	2.23[+33]	2.31[+34]	2.38[+35]	2.46[+36]
2.60[+38]	2.74[+40]	2.88[+42]	3.02[+44]	3.17[+46]	3.32[+48]	3.50[+50]	4.02[+55]

Note. — The complete version of this table can be found in the electronic edition of Astrophysical Journal Supplement. The printed edition contains only a sample of what kind of information is given. The full tables can also be downloaded from http://ftp.nucastro.org/astro/fits/partfuncs/.